

Interference of harmonics emitted by different tunneling momentum channels in laser fields

Ling-Yu Zhang(张玲玉), Zhuo-Xuan Xie(谢卓璇), Can Wang(王灿), Xin-Lei Ge(葛鑫磊), and Jing Guo(郭静)
Citation: Chin. Phys. B, 2024, 33 (**9**): 093201. DOI: 10.1088/1674-1056/ad5d95
Journal homepage: http://cpb.iphy.ac.cn; http://iopscience.iop.org/cpb

What follows is a list of articles you may be interested in

Role of excited states in helium-like ions on high-order harmonic generation

Jiang-Hua Luo(罗江华) and Jia-Jun Xiao(肖佳俊)
Chin. Phys. B, 2023, 32 (**11**): 113201. DOI: 10.1088/1674-1056/ace317

Phase-coherence dynamics of frequency-comb emission via high-order harmonic generation in few-cycle pulse trains

Chang-Tong Liang(梁畅通), Jing-Jing Zhang(张晶晶), and Peng-Cheng Li(李鹏程)
Chin. Phys. B, 2023, 32 (**3**): 033201. DOI: 10.1088/1674-1056/acac0f

High-order harmonic generation of the cyclo[18]carbon molecule irradiated by circularly polarized laser pulse

Shu-Shan Zhou(周书山), Yu-Jun Yang(杨玉军), Yang Yang(杨扬), Ming-Yue Suo(索明月), Dong-Yuan Li(李东垣), Yue Qiao(乔月), Hai-Ying Yuan(袁海颖), Wen-Di Lan(蓝文迪), and Mu-Hong Hu(胡木宏)
Chin. Phys. B, 2023, 32 (**1**): 013201. DOI: 10.1088/1674-1056/aca3a1

Probing subcycle spectral structures and dynamics of high-order harmonic generation in crystals

Long Lin(林龙), Tong-Gang Jia(贾铜钢), Zhi-Bin Wang(王志斌), and Peng-Cheng Li(李鹏程)
Chin. Phys. B, 2022, 31 (**9**): 093202. DOI: 10.1088/1674-1056/ac6943

Generation of elliptical isolated attosecond pulse from oriented H_2^+ in a linearly polarized laser field

Yun-He Xing(邢云鹤), Jun Zhang(张军), Xiao-Xin Huo(霍晓鑫), Qing-Yun Xu(徐清芸), and Xue-Shen Liu(刘学深)
Chin. Phys. B, 2022, 31 (**4**): 043203. DOI: 10.1088/1674-1056/ac398b

---

Interference of harmonics emitted by different tunneling momentum channels in laser fields

Ling-Yu Zhang(张玲玉)[1], Zhuo-Xuan Xie(谢卓璇)[1], Can Wang(王灿)[1], Xin-Lei Ge(葛鑫磊)[2], and Jing Guo(郭静)[1,†]

[1] *Institute of Atomic and Molecular Physics, Jilin University, Changchun* 130012, *China*
[2] *College of Physical Science and Technology, Bohai University, Jinzhou* 121013, *China*

(Received 21 May 2024; revised manuscript received 1 July 2024; accepted manuscript online 2 July 2024)

By numerically solving the semiconductor Bloch equation (SBEs), we theoretically study the high-harmonic generation of ZnO crystals driven by one-color and two-color intense laser pulses. The results show the enhancement of harmonics and the cut-off remains the same in the two-color field, which can be explained by the recollision trajectories and electron excitation from multi-channels. Based on the quantum path analysis, we investigate contribution of different ranges of the crystal momentum k of ZnO to the harmonic yield, and find that in two-color laser fields, the intensity of the harmonic yield of different ranges from the crystal momentum makes a big difference and the harmonic intensity is depressed from all k channels, which is related to the interferences between harmonics from symmetric k channels.

Keywords: high-order harmonic generation, the semiconductor Bloch equation, k-resolved inter-band harmonic spectrum, four-step semiclassical model

PACS: 32.80.Rm, 42.65.Ky, 42.65.Re **DOI:** 10.1088/1674-1056/ad5d95

1. Introduction

As a new attosecond light source, high harmonic generation (HHG) has been a hot topic in recent decades,[1–5] which can produce intense and short attosecond pulses. There are a series of work on the contribution of different bands in the solids,[6–8] intraband and interband contributions,[9] temporal restriction of inter-band excitation by intra-band motion,[10] the contribution of multiple channels,[11,12] and contributions from the initial state including only the $k = 0$ point or that including the entire first Brillouin zone (BZ).[13,14] At present, the intraband current and interband polarization are the main mechanisms of high harmonic generation in solids, and there are couplings between these two mechanisms, which not only affects the injection of the electron from valence band to conduction band, but also affects the motion of electrons in the momentum space from the conduction band.[10,15,16] Based on the semi-classical three-step model of gas, the recollision model of HHG in solids is proposed.[17,18] First, when the intense laser interacts with the solids, the electrons tunnel near the top of the valence band and leaving the hole in the valence band; then the electrons and holes are accerlated in intense laser fields, finally, the electron and hole will be recombined with a certain probability to emit high harmonics.

Li *et al*.[19] proposed a four-step model to study solid HHG, which further improved the physical process of high harmonic generation in solids. Compared with the three-step model, there was a pre-acceleration process, and some electrons were pre-accelerated to near the top of the valence band before ionization. However, in previous studies of HHG in solid, it is generally believed that most electrons are excited by tunneling near the top of the valence band. However, recent studies have shown that electrons are not only excited by tunneling in a small band gap, but also probably far from the top of the valence band. Sun *et al*. proposed the extension of the cutoff in HHG by the resonant electron injection channels.[20] Du found theoretically that the temporal properties and yield of the high harmonics sensitively depend on the crystal momentum region generating electron–hole pairs.[21] In the previous studies, people investigated the initial state only including $k = 0$ point or including the first Brillouin zone,[13,14] and also studied the contribution of the various ranges of tunneling momentum k in high harmonic generation,[21,22] but the comparison between hamonics from different ranges of tunneling momentum k and their physical picture is few, and the interference effect from which still needs further exploration. Moreover, some recent studies have demonstrated that the interference between the interband currents affects the radiation of the crystal harmonic spectrum,[23] and that changing the relative phase of the two-color circular polarization field can modulate the plateau harmonic intensity.[24] Therefore, in this paper, we study the HHG of ZnO crystals driven by linear polarized one-color and two-color laser pulses by numerically solving the semiconductor Bloch equation. Based on the quantum path analysis of the structural characteristics of the harmonics by two laser pulses, we investigated the influence of different tunneling momentum regions on the harmonics in solids, and the different interferences between symmetric channels of the

†Corresponding author. E-mail: gjing@jlu.edu.cn

© 2024 Chinese Physical Society and IOP Publishing Ltd

crystal momentum k.

In this paper, the Section 2 is the theoretical method we use, and our results and analysis are presented in Section 3. Atomic unit is used unless otherwise stated.

2. Theoretical method

The theoretical method we adopted is to numerically solve the semiconductor Bloch equation (SBEs)[25–27] as follows:

$$\begin{aligned}\dot{\pi}_{mm'} &= -\frac{\pi_{mm'}}{T_2} + \mathrm{i}\Omega^*_{mm'}(n_m - n_{m'})\,\mathrm{e}^{-\mathrm{i}S_{mm'}} \\ &\quad + \mathrm{i}\sum_{m''\notin\{m,m'\}}(\Omega_{m'm''}\pi_{mm''}\,\mathrm{e}^{\mathrm{i}S_{m'm''}} \\ &\quad - \Omega^*_{mm''}\pi^*_{m'm''}\,\mathrm{e}^{-\mathrm{i}S_{mm''}}), \qquad (1)\\ \dot{n}_m &= \mathrm{i}\sum_{m'\neq m}\Omega_{mm'}\pi_{mm'}\,\mathrm{e}^{\mathrm{i}S_{mm'}} + \mathrm{c.c.}, \qquad (2)\end{aligned}$$

where $\pi_{mm'}(\boldsymbol{K},t)$ is the diagonal element of the density matrix, $\boldsymbol{K}(t)$ is time-dependent momentum, $\boldsymbol{K}(t)=\boldsymbol{k}-\boldsymbol{A}(t)$, $\boldsymbol{k}$ is initial momentum. n_m is the population in the m-th band, T_2 is the dephasing time. $\Omega_{mm'}(\boldsymbol{K},t)=\boldsymbol{E}(t)\cdot d_{mm'}[\boldsymbol{K}+\boldsymbol{A}(t)]$ is the Rabi frequency, where $\boldsymbol{E}(t)$ is the electric field and $d_{mm'}[\boldsymbol{K}+\boldsymbol{A}(t)]$ is the momentum-dependent transition dipole moment of the crystal between the two bands. $\mathrm{e}^{\mathrm{i}S_{mm'}}$ is the phase term, and $S_{mm'}(\boldsymbol{K},t)=\int_{-\infty}^{t}\{\varepsilon_m[\boldsymbol{K}+\boldsymbol{A}(t')]-\varepsilon_{m'}[\boldsymbol{K}+\boldsymbol{A}(t')]\}\,\mathrm{d}t'$ is the classical action, and ε_m and $\varepsilon_{m'}$ refer to band energies.

By solving SBEs, we can calculate the induced intraband and interband currents as follows:[5]

$$\boldsymbol{j}_{\mathrm{ra}}(t)=\sum_m\int_{\bar{BZ}}\boldsymbol{v}_m[\boldsymbol{K}+\boldsymbol{A}(t)]n_m(\boldsymbol{K},t)\,\mathrm{d}^3\boldsymbol{K}, \qquad (3)$$

$$\boldsymbol{j}_{\mathrm{er}}(t)=\frac{\mathrm{d}}{\mathrm{d}t}\sum_{m\neq m'}\int_{\bar{BZ}}\boldsymbol{p}_{mm'}(\boldsymbol{K},t)\,\mathrm{d}^3\boldsymbol{K}, \qquad (4)$$

where

$$\boldsymbol{p}_{mm'}(\boldsymbol{K},t)=d_{mm'}(\boldsymbol{K},t)\pi_{mm'}(\boldsymbol{K},t)\,\mathrm{e}^{\mathrm{i}S_{mm'}(\boldsymbol{K},t)}+\mathrm{c.c.}$$

represents the polarizability between two energy bands. $\boldsymbol{v}_m(\boldsymbol{k})=\nabla_{\boldsymbol{k}}\varepsilon_m(\boldsymbol{k})$ denotes the velocity of the m-th band. $\boldsymbol{A}(t)$ is the vector potential. The harmonic spectra are obtained by taking the Fourier transform of the current

$$I_{\mathrm{HHG}}(\omega)=|\omega\mathrm{FFT}[j_{\mathrm{ra}}(t)+j_{\mathrm{er}}(t)]|^2. \qquad (5)$$

The laser field we used is as follows:

$$E(t)=f_0(t)E_0\cos(\omega_0 t)+f_1(t)E_1\cos[\omega_1(t-t_{\mathrm{d}})], \qquad (6)$$

where the Gaussian envelopes are

$$f_0(t)=\exp\left[-2(\ln 2)\frac{t^2}{\tau_0^2}\right], \qquad (7)$$

$$f_1(t)=\exp\left[-2(\ln 2)\frac{(t-t_{\mathrm{d}})^2}{\tau_1^2}\right]. \qquad (8)$$

We chose the laser intensity 5×10^{11} W/cm^2 with wavelength of 3005 nm, and the laser intensity 7×10^{10} W/cm^2 with wavelength of 334 nm, the total duration of laser is 25 o.c. (optical cycle).

To reveal the properties of the k-resolved HHG spectra and the effects between different channels which emit harmonics, we sampled Brillouin regions (BZ) $[-\pi/a,\pi/a]$ using 401 equally-spaced k-points, where $a=5.32$ is the lattice constant in the Γ–M direction and each k-point is defined as a specific n-channel ($n=-200,-199,\ldots200$).

3. Results and discussion

First, we present the harmonic spectra driven by the one-color and the two-color linearly polarized laser fields (Fig. 1(a)), the population of the conduction band as functions of time (Fig. 1(b)), and the intensity of k-resolved harmonics (Figs. 1(c) and 1(d)). As can be seen in Fig. 1(a), compared with the one-color field, the harmonic intensity is increased about 2–4 orders of magnitude, and the harmonic spectrum presents a discrete peak structure, and the peaks are broadened, the modulation is reduced, but the cutoff is almost the same, and by intensity of k-resolved harmonics (Figs. 1(c) and 1(d)), we can see that in case of one-color field, the intensity is symmetric about $k=0$, whereas in the two-color field, the intensity are strong in the left and weak in the right for some symmetric channels. And for the harmonics in the plateau region (such as the harmonics larger than the 12th order), the harmonic intensity of the $k<0$ interval is significantly stronger than that of the $k>0$ interval. This can be further illustrated by population of the electrons on the conduction band. Figure 1(b) shows that the electron located at $t=0$ o.c. is rapidly excited in a cycle, which is also an important factor of harmonic enhancement. Furthermore, we want to understand the physical pictures and the reason of the enhancement, so we have done the follow-up investigation.

By calculating the harmonics at the smallest band gap $n=0$ and smaller band gap $n\in[20,20]$ in Fig. 2, we can find that in the two-color field, the intraband harmonics is about 2–4 orders of magnitude higher than that of one-color field (Fig. 2(a)), and except for H11 (11th harmonic), H13, and H15, the interband harmonic intensity is almost the same as that in one-color field (Fig. 2(b)). Since we used mid-infrared field in this paper, and in this frequency the interband harmonics is dominant (much higher than intraband harmonics), thus, the total harmonics is almost the same as that in one-color field except for H11, H13, and H15 (Fig. 2(c)). Besides, the total harmonic intensity from the range $n\in[20,20]$ is much greater than that of $n=0$ in both one-color and two-color fields in Fig. 2. This shows that besides near the valence band top, other ionization channels contribute greatly to the enhancement of harmonics.

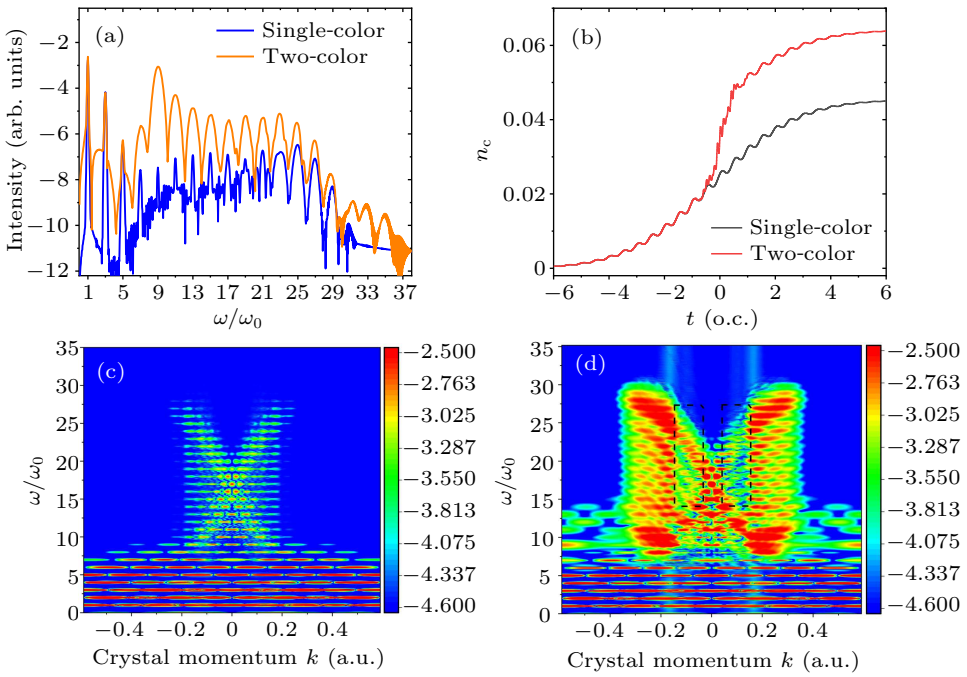


Fig. 1. (a) The harmonic spectra generated by the ZnO crystal driven by the one-color and two-color linearly polarized laser fields, (b) the population of conduction band as functions of time, (c) the k-resolved harmonic spectrum in one-color field, and (d) the k-resolved harmonic spectrum in the two-color field.

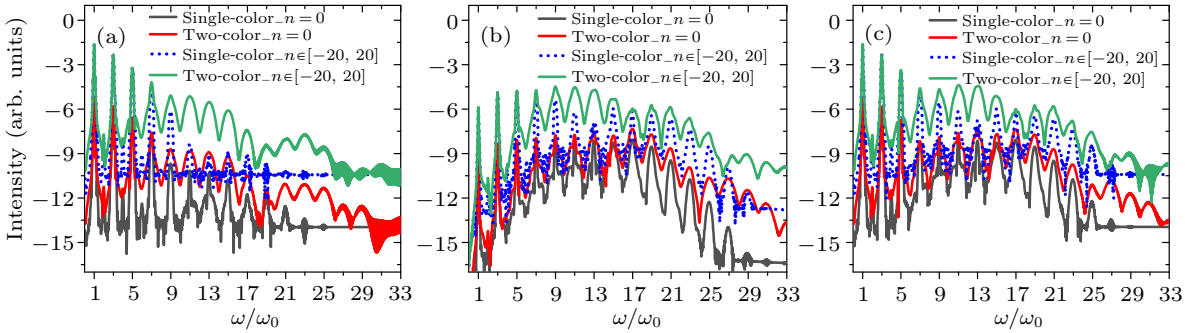


Fig. 2. (a) Intraband harmonic spectra, (b) interband harmonic spectra, and (c) total harmonic spectra at $n = 0$ and $n \in [20, 20]$ interval in the one-color and two-color fields.

In order to reveal the physical root of the large enhancement of plateau in harmonics, we study the motion of electrons and holes, which can be further analyzed by the recollision trajectories of real space and reciprocal space (k space).

Figure 3 shows the trajectory of the ionized electron in momentum space at time $t = 0.1$ o.c. and distance between the electron and hole in real space as functions of time. According to Bloch's acceleration theorem $\boldsymbol{K}(t) = \boldsymbol{k} - \boldsymbol{A}(t)$, the k space trajectory of the electron (hole) is obtained as $\boldsymbol{k}(t) = \boldsymbol{K}' + \boldsymbol{A}(t) = \boldsymbol{k}_0 - \boldsymbol{A}(t') + \boldsymbol{A}(t)$, where $\boldsymbol{A}(t)$ is the vector potential, and vector potential of one-color field and two-color field change with the same tendency, and the amplitude difference of electric field is small, as shown in Fig. 3, the k space trajectory are almost the same, the range of bloch oscillation from electrons and holes is not big, and by saddle point conditions of energy conservation, i.e., the photon energy of harmonics equal to the instantaneous band gap of recollision between electron and hole. Therefore, driven by one-color and two-color laser pulses, the resulting frequency of harmonic cutoff are close (see Fig. 1(a)).

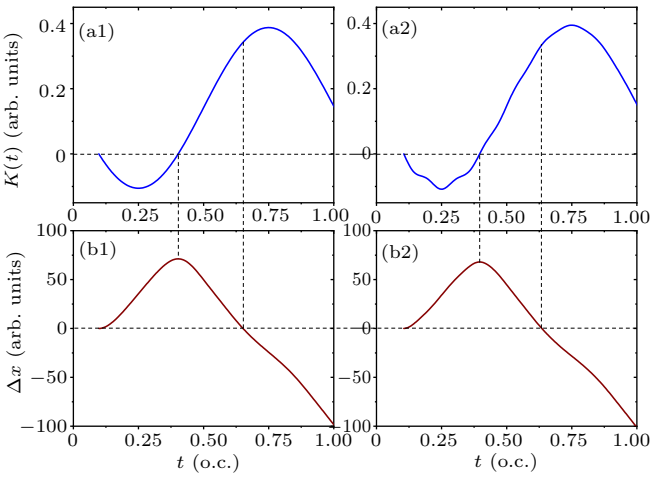


Fig. 3. By one-color [(a1), (b1)] and two-color [(a2), (b2)] linearly polarized fields, the trajectory of ionized electrons at $t = 0.1$ o.c. in k space and distance between the electron and the hole in real space as functions of time.

Moreover, the close cut-off energy of the harmonic spectrum in the two-color field and the one-color field can also be analyzed by formula for the cut-off energy. The cutoff energy of harmonic spectrum is as follows:[28]

$$\Omega_{\text{cutoff}} = E_{\text{g}} + (\Delta c + \Delta v)\left[1 - \frac{\pi}{2} + a_x \frac{F_0 \delta}{\omega}\right], \tag{9}$$

where E_{g} is the minimum band gap between the nearest neighbor bands, $\Delta c = 0.0872$ a.u., $\Delta v = 0.0925$ a.u., $a_x = 2\pi/k_x$ is the lattice constant of the zinc oxide crystal along the Γ–M direction, F_0 is the peak intensity of the laser field, ω is the angular frequency of the laser field, δ is the term related to the tunneling time and recollision time. It can be found from the formula that the cut-off energy is related to the amplitude and angular frequency of the laser field. The amplitude of the fundamental field is $F_0 = 0.003775$ a.u., and angular frequency is $\omega = 0.0152$ a.u., and the peak power of the second laser is $F_1 = 0.001412$ a.u., angular frequency is $\omega_1 = 0.1364$ a.u. F_1/ω_1 is an order of magnitude smaller than F_0/ω, so $F_0/\omega + F_1/\omega_1 \approx F_0/\omega$. Therefore, the cutoff frequency of the harmonic spectrum in the two-color field is almost the same that in the one-color field.

Based on the motion of the electron and hole, combined with the instantaneous population of conduction band (CB) to further analyze the enhancement of harmonic intensity. In the case of one-color field, there is a peak in the half period of the laser field with maximum electric field strength (Fig. 4(b)), which mainly corresponds to the tunneling excitation, corresponding to the single channel ionization presented by the instantaneous population of conduction band in Figs. 4(a) and 4(c). The motion of electrons (as shown in Fig. 4(d)) can be described as: when the laser field reaches the peak and the vector potential is 0, the electrons moving to near the top of the valence band by pre-acceleration process reach the conduction band; then the electrons on conduction band undergo Bloch oscillations, emiting intraband harmonics. Finally part of the electrons return to the valence band and recombine with holes, and emit interband harmonics.

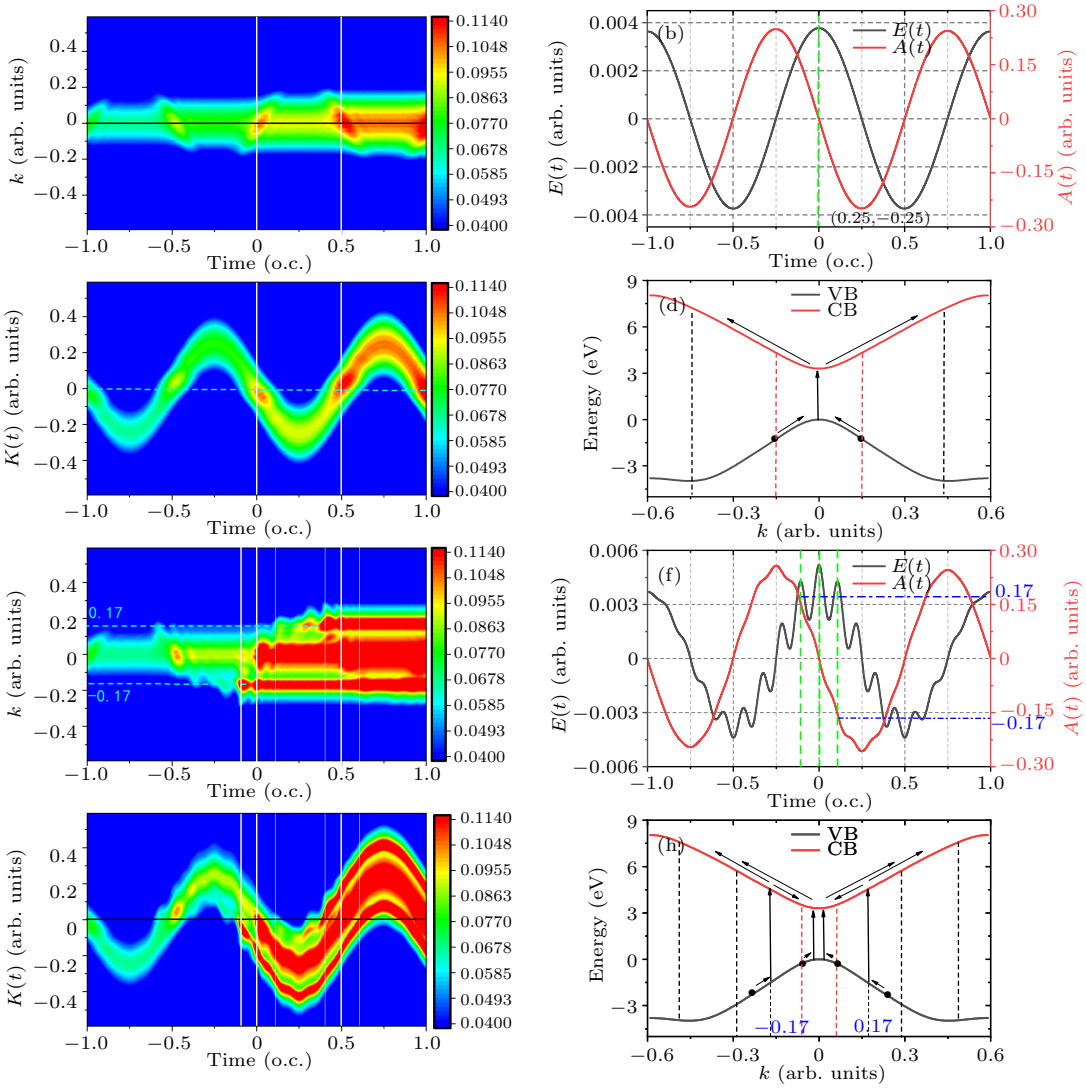


Fig. 4. (a) The instantaneous population of conduction band as functions of the initial momentum k and time t, (b) the one-color laser field and the vector potential, (c) the instantaneous population of conduction band as a function of the time-dependent crystal momentum $\boldsymbol{K}(t)$, and (d) the schematic diagram of the electron motion in k space in one-color laser field. Panels (e)–(h) are the corresponding cases in the two-color field.

However, the two-color field has three large values in the half period which includes the peak of electric field (Fig. 4(f)), which mainly corresponds to the three times rapid excitation of electrons, corresponding to the three ionization channels in Figs. 4(e) and 4(g), and the ionized electrons undergo Bloch oscillations and superimposed, as shown in Fig. 4(g). The resonant electron injection channels can be explained by the conditions of ionization excitation.

We know that the fast excitation of resonant electron injection into the three ionization channels also satisfies the excitation conditions for the tunneling ionization channel. When the laser field reaches three peak values, the corresponding vector potentials are −0.17 a.u., 0 a.u., 0.17 a.u., respectively. Since the tunneling excitation of electrons satisfies the crystal momentum $\boldsymbol{K}' = 0$, according to $\boldsymbol{K}' = \boldsymbol{k} - \boldsymbol{A}(t')$, we know that in the two-color field case, the ionization channel corresponds to $k = -0.17$ a.u., 0 a.u., 0.17 a.u. The generation of multiple channels corresponds to three times electron bursts excited in the half period of the laser field, and the population of conduction band is rapidly increased, and then driven by the intense laser field, more electrons return to the valence band, and the intraband and interband harmonics are enhanced, so the intensity of the total harmonics is increased.

The analysis of quantum paths and their interference in high harmonic generation has been investigated in many researches, and the contribution of long trajectory and its interference[29,30] with short trajectory have been confirmed. In order to clearly understand the factors affecting the difference in the harmonic spectral structure driven by one-color and two-color laser pulses, we present the time-frequency distribution, recollision model and the corresponding electron population of conduction band and analyze them accordingly.

We can see from the time-frequency distribution of the harmonics that the harmonic intensity is higher in two-color field than that in one-color field (see Figs. 5(a) and 5(b)). Furthermore, in the case of two-color laser field, the contribution of short trajectory is stronger, while the long trajectory is suppressed and its contribution is almost negligible. Therefore, the modulation of corresponding harmonics by the two-color field in Fig. 1(a) is reduced, and the peak of harmonics is broadened.

Based on electron population as functions of time and the recollision model, it can be found that compared with the case of one-color laser field, more electrons are ionized by the two-color laser pulse, the time corresponding to the three burst excitation ionization is $t = -0.5$ o.c., 0 o.c., 0.5 o.c. Furthermore, even more electrons may return to the valence band and recombined with hole and emit high-energy photons (as shown in Figs. 5(c) and 5(d)). Therefore, in the case of two-color field, the harmonic intensity is stronger, which also corresponds to the strength of the harmonics in Figs. 5(a) and 5(b).

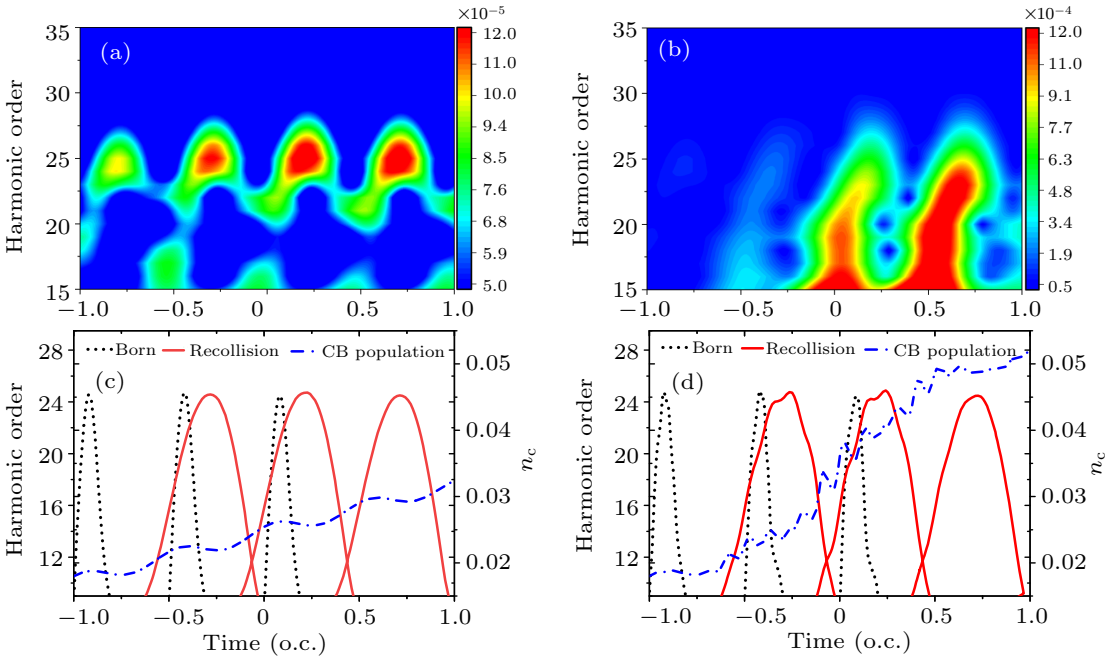


Fig. 5. Time-frequency analysis of harmonics in (a) one-color and (b) two-color fields; (c) harmonics as functions of ionization time and return time in (c) one-color and (d) two-color fields.

We then investigate the harmonics emitted from different range of tunneling momentum k by one-color and two-color fields respectively. The range of momentum with tunneling[21,31,32] can be controlled experimentally by the impurity of photon carrier using the appropriate laser pulse. In our study, we find that the harmonics emitted from different momentum ranges show intensity differences, and there is a critical momentum range in which the harmonic intensity is the strongest, and beyond this range the harmonic intensity is suppressed. In Fig. 6, we present harmonic spectra of the mo-

mentum range of $n \in [-68,68]$ and $n \in [-200,200]$ driven by a two-color laser field. It is found that the harmonic intensity of all channels is suppressed by the two-color field, and the harmonic intensity of the range $n \in [-68,68]$ is higher than that of the all-channel.

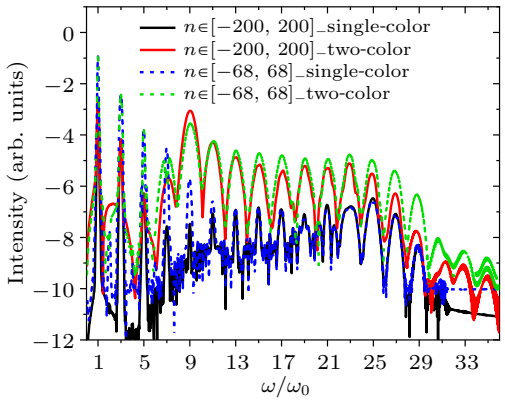


Fig. 6. Harmonics from the range of $n \in [-68,68]$ and $n \in [-200,200]$ by a one-color field and two-color laser field.

To understand the reason why the intensity of the harmonic plateau with full channels is suppressed in the two-color field, we investigate the contribution of different ranges of momentum channels to the time-frequency distribution. Because the interband harmonics contribute mainly to the plateau of the harmonic spectrum, so we present the time-frequency of the radiation harmonics of range $n \in [-68,68]$ and $n \in [-200,200]$ in one-color and two-color fields, In one-color field (Figs. 7(a1) and 7(b1)), the harmonic intensity of ranges $n \in [-68,68]$ and $n \in [-200,200]$ are almost the same. However, in the case of two-color field (as shown in Figs. 7(a2) and 7(b2)), there are large differences between $n \in [-68,68]$ and $n \in [-200,200]$. Since the main contribution comes from short trajectory, so the weakening of the harmonic intensity is unrelated to the quantum path interference; and at $t = 0$ o.c., the harmonic emitted from all-channel is mostly suppressed.

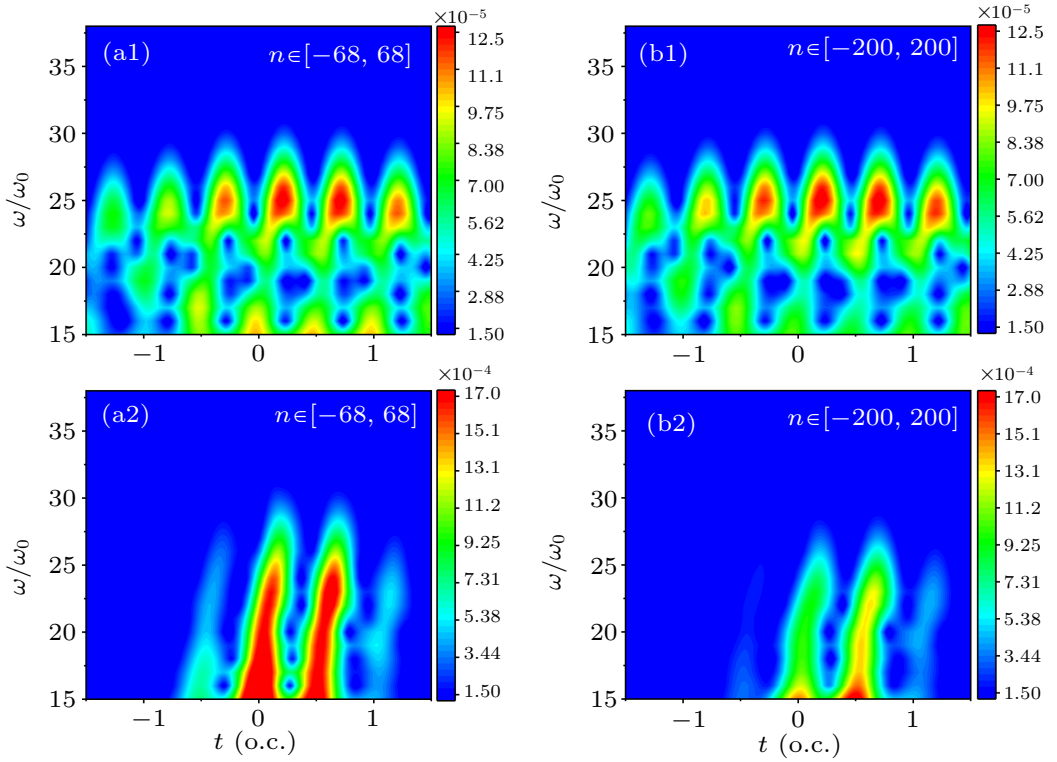


Fig. 7. Time–frequency analysis of the interband harmonics between $n \in [-68,68]$ and $n \in [-200,200]$ in (a1)–(b1) one-color and (a2)–(b2) two-color fields.

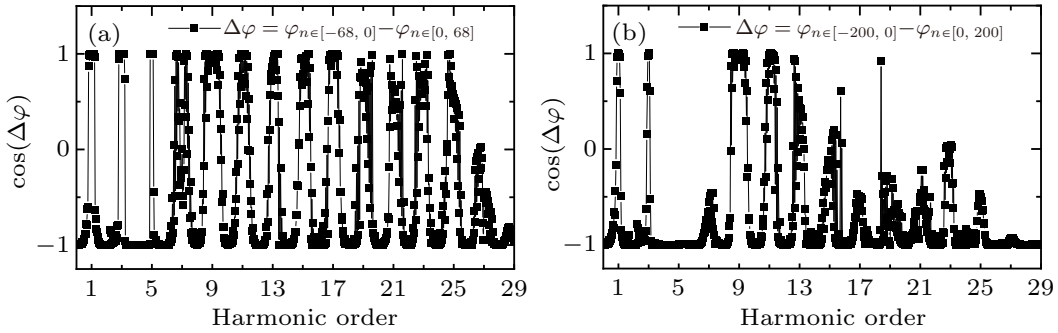


Fig. 8. In two-color fields, (a) the cosine of the phase difference between symmetric ranges $n \in [-68,0]$ and $n \in [0,68]$;(b) the cosine of the phase difference between symmetric ranges $n \in [-200,0]$ and $n \in [0,200]$.

In previous research, it was demonstrated that harmonics below the band gap originate from the interference between intra-band and inter-band currents[33] and odd harmonic in symmetric channels was constructive interference, while even harmonic was destructive interference.[26] However, there is little research on the phase difference between the total harmonics. Therefore, we further calculated the cosine value of the phase difference between the total harmonics emitted from the symmetric channels (as shown in Fig. 8), and the results showed that in Fig. 8(a), the cosine value of the phase difference between the total harmonics emitted from the symmetric ranges $n \in [-68,0]$ and $n \in [0,68]$ indicates that the harmonic with constructive interference is roughly equal to the harmonic with destructive interference; The cosine value of the phase difference between the total harmonic radiation in the symmetric ranges $n \in [-200,0]$ and $n \in [0,200]$ indicates that the harmonics with destructive interference is much more than the harmonic with constructive interference, so destructive interference dominates. Compared to the situation where the total harmonic with destructive interference and constructive interference are roughly equivalent in $n \in [-68,0]$ and $n \in [0,68]$, it can be concluded that the harmonic intensity of range $n \in [-200,200]$ is lower than that of range $n \in [-68,68]$.

4. Conclusion

In summary, we theoretically investigate the high harmonic generation of ZnO crystals driven by one-color and two-color intense laser pulses. The results show that the excitation of the electron is enhanced with two-color fields. Through the analysis of the instantaneous population of conduction band, it is found that the dynamics of electron–hole pairs can well explain the enhancement of harmonics and the phenomenon of keeping the cutoff frequency of the harmonic spectrum unchanged. Based on the quantum path analysis, the contribution of different tunneling channels to the harmonic generation in ZnO crystals by two-color field was studied. It was found that the strength of the harmonic emitted by symmetric channels from different ranges has large difference. Compared with the harmonics emitted by tunneling momentum channels range from $n \in [-68,68]$, the intensity of harmonics was suppressed when considering the full channel $n \in [-200,200]$. Through analysis, it is found that this is related to the interference between the harmonics in symmetric channels in different momentum ranges.

Acknowledgments

Project supported by the National Natural Science Foundation of China (Grant No. 12074146) and the Natural Science Foundation of Jilin Province, China (Grant No. 20220101010JC).

References

[1] Li J, Lu J, Chew A, Han S, Li J L, Wu Y, Wang H, Ghimire S and Chang Z H 2020 *Nat. Commun.* **11** 2748
[2] Krause J L, Schafer K J and Kulander K C 1992 *Phys. Rev. Lett.* **68** 3535
[3] Ghimire S, DiChiara A D, Sistrunk E, Agostini P, DiMauro L F and Reis D A 2011 *Nat. Phys.* **7** 138
[4] Zhang H D, Liu X W, Jin F C, Zhu M, Yang S D, Dong W H, Song X H and Yang W F 2021 *Chin. Phys. Lett.* **38** 063201
[5] Vampa G, McDonald C R, Orlando G, Klug D D, Corkum P B and Brabec T 2014 *Phys. Rev. Lett.* **113** 073901
[6] Wu M X, You Y S, Ghimire S, Reis D A, Browne D A, Schafer K J and Gaarde M B 2017 *Phys. Rev. A* **96** 063412
[7] Lang Y, Peng Z Y and Zhao Z X 2022 *Chin. Phys. Lett.* **39** 114201
[8] Lang Y, Peng Z Y, Liu J L, Zhao Z X and Ghimire S 2022 *Phys. Rev. Lett.* **129** 167402
[9] Golde D, Meier T and Koch S W 2008 *Phys. Rev. B* **77** 075330
[10] Song X H, Zuo R X, Yang S D, Li P C, Meier T and Yang W F 2019 *Opt Express.* **27** 2225
[11] Du T Y, Tang D, Huang X H and Bian X B 2018 *Phys. Rev. A* **97** 043413
[12] Song X H, Yang S D, Wang G F, Lin J H, Wang L, Meier T and Yang W F 2023 *Opt. Express* **31** 18862
[13] Jin J Z, Liang H, Xiao X R, Wang M X, Chen S G, Wu X Y, Gong Q H and Peng L Y 2019 *Phys. Rev. A* **100** 013412
[14] Navarrete F, Ciappina M F and Thumm U 2020 *J. Phys. Conf. Ser.* **1412** 082006
[15] Schlaepfer F, Lucchini M, Sato S A, Volkov M, Kasmi L, Hartmann N, Rubio A, Gallmann L and Keller U 2018 *Nat. Phys.* **14** 560
[16] Zhao J, Liu J L, Wang X W, Yuan J M and Zhao Z X 2022 *Chin. Phys. Lett.* **39** 123201
[17] Vampa G and Brabec T 2017 *J. Phys. B-At Mol. Opt.* **50** 083001
[18] Fu S L, Feng Y K, Li J B, Yue S J, Zhang X, Hu B T and Du H C 2020 *Phys. Rev. A* **101** 023402
[19] Li L, Lan P F, Zhu X S, Huang T F, Zhang Q B, Lein M and Lu P X 2019 *Phys. Rev. Lett.* **122** 193901
[20] Sun N, Zhu X S, Li L, Lan P F and Lu P X 2021 *Phys. Rev. A* **103** 053111
[21] Du T Y 2021 *Phys. Rev. A* **104** 063110
[22] Zhang C P and Miao X Y 2023 *Chin. Phys. Lett.* **40** 124201
[23] Qiao Y, Chen J Q, Huo Y Q, Liang H Q, Yu R X, Chen J G, Liu W J, Jiang S C and Yang Y J 2023 *Phys. Rev. A* **107** 023523
[24] Qiao Y, Chen J Q, Zhou S S, Chen J G,Jiang S C and Yang Y J 2024 *Chin. Phys. Lett.* **41** 014205
[25] Yu C, Jiang S C and Lu R F 2019 *Adv. Phys. X* **4** 1562982
[26] He Y L, Guo J, Gao F Y, Yang Z J, Zhang S Q and Liu X S 2021 *Phys. Rev. A* **104** 013104
[27] Wu D, Li L, Zhan Y T, Huang T F, Cui H B, Li J P, Lan P F and Lu P X 2022 *Phys. Rev. A* **105** 063101
[28] Vampa G, McDonald C R, Orlando G, Corkum P B and Brabec T 2015 *Phys. Rev. B* **91** 064302
[29] Zaïr A, Holler M, Guandalini A, Schapper F, Biegert J, Gallmann L, Keller U, Wyatt A S, Monmayrant A, Walmsley I A, Cormier E, Auguste T, Caumes J P and Salières P 2008 *Phys. Rev. Lett.* **100** 143902
[30] Shao T J, Lü L J, Liu J Q and Bian X B 2020 *Phys. Rev. A* **101** 053421
[31] Wang Z, Park H, Lai Y H, Xu J L, Blaga C I, Yang F Y, Agostini P and DiMauro L F 2017 *Nat. Commun.* **8** 1686
[32] Heide C, Kobayashi Y, Johnson A, Liu F, Heinz T, Reis D A and Ghimire S 2022 *CLEO* FF4N.5
[33] Zhao Y T, Jiang S C , Zhao X, Chen J G and Yang Y J 2020 *Opt. Lett.* **45** 2874